CHAPTER II

THEORY AND LITERATURE REVIEWS

2.1 Structure of perovskites

2.1.1 Crystal structure

The ideal perovskite-type structure is cubic, generally used for metal oxides with the sum formula of perovskite-type oxides ABO_3, where A is the larger twelve coordinated cation and B is the smaller six coordinated cation. The oxidation number of the A cation ranges from +1 to +3, and the oxidation number of the B cation from +3 to +6. Whereas the ideal structure is cubic, the actual structure is often disturbed. Alternatively, the structure can be viewed with the B cation in the center and the A cation is in the center of the cube, as shown in Figure 2.1. B is surrounded by an oxide ion octahedron.

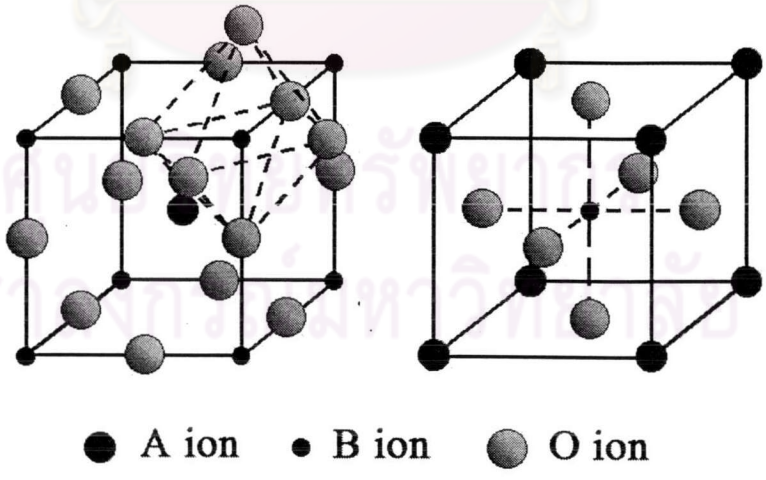

Figure 2.1 ABO_3 ideal perovskite structure showing oxygen octahedron containing the B ion linked through corners to form a three-dimensional cubic lattice.

The formation of perovskite-oxides with high oxygen ionic conductivity requires high oxygen vacancy concentrations created by dopants, and best conditions for oxygen mobility. The ionic radii of the dopants must be fitted to the lattice, while is expressed by the Goldschmidt tolerance factor: [13]

$$t = (r_A + r_O) / \sqrt{2(r_B + r_O)} \qquad (2.1)$$

Where the atoms are touching one another, the B-O distance is equal to $a/2$ (a is the cubic unit cell parameter) while the A-O distance is $(a/\sqrt{2})$ and the following relationship between the ionic radius (r) holds: $r_A + r_O = \sqrt{2(r_B + r_O)}$. In general, the perovskite structure is formed if the tolerance factor, t, is in the range 0.75-1.0 results in an undistorted cubic perovskite structure.

The indices A, B and O mark the structure-sites of the perovskite oxide ABO_3. Only a t-factor near unity (1.0 - 0.95) results in an undistorted cubic perovskite structure of high oxygen mobility (highest number of crystallographically equipvalent oxygen sites) [14]. For tolerance factors of 0.90 - 0.75 in many cases an orthorhombic perovskite structure is formed, which is for oxygen ionic mobility an acceptable structure too.

Additional doping on the A and B sites makes it easy to change the electrical characteristics of perovskite type oxides. Although some of the rules of the doping/property relations are known, most of the developments of new material compositions of interest for practical application were more or less empirical. Recently, formation of the perovskite structure requires ionic radii fitting to the lattice, expressed by the Goldschmidt number t. Only a t value near unity results in a cubic perovskire structure, whereas greater declinations from unity give distorted unit cells. It was observed that high oxygen ionic conductivity correlates with a cubic or orthorhombic structure [15]. Additionally, Yokokawa [16-17] observed a strong correlation between the formation of perovskite phases from oxides and the Goldschmidt numbers. Thermodynamic stability increases with increasing Goldschmidt number. This correlation helps to establish doping strategies, calculating with mean ionic radii in the case of doping.

2.1.2 Nonstoichiometry in perovskites

Nonsoichiometry in perovskite can arise from either cation or anion deficiency (in the A or B site). Due to the partial substitution of A and B ions giving rise to complex oxides has to keep the perovskite structure. For the A-site cations deficiency [18], it can be missing without collapse of the perovskite network because of the stability of the BO_3 group. The B-site vacancies are not favorites to energetically because of the large formal charge and the small size of the B cations in perovskites. Nevertheless, an oxygen vacancy in perovskites is more common than a cation deficiency.

However, description of oxygen-deficient perovskites can be used by the basis of complex perovskite-related super-structures of general formula $A_nB_nO_{3n-1}$. It can be the stacking manner depends on the size, electronic configurations, and coordination numbers of A and B cations. The substitutions of ions with similar sizes but different valence were accomplished to generate oxygen vacancies. For example, some of the La^{3+} ions in $LaBO_3$ are replaced by Sr^{2+} to form $La_{1-x}Sr_xBO_{3-\delta}$, and therefore, oxygen vacancies are formed in the structure.

2.2 Physical properties

For characterization of the perovskite materials, it is more often to measure their electronic and ionic conductivity instead of concentrations of electrons (holes) and mobile ions (vacancy). The calculated ionic and electronic conductivity, are measured by using dc 4-probe technique.

In the ideal cubic perovskite structure, which is facilitated by overlap between B lattice cations and O^{2-} orbital occurs via B-O-B bonds angle at 180 °C. In the orthorhombic structure, the tilting of BO_6 octahedral gives rise to a larger barrier to electron conduction. Therefore, the electronic conduction requires the presence of B site cations with multiple valences. The physical properties of perovskite iron oxides are related to the network of FeO_6. It is known that the properties of these types of oxides are affected by the number of layers of FeO_6 octahedra. The charge disproportionation ($2Fe^{+4} \rightarrow Fe^{+3} + Fe^{+5}$) not observed in SrFeO3; occurs in the oxides being cut the network of Fe^{+4} O_6 octahedra, for example, by introduction of

Fe^{+3} by substitution La for Sr and change in the dimension by insertion of SrO layer . When Co is substituted 40% of Fe in $Sr_3Fe_2O_7$; the magnetic order changes to ferromagnetic from antiferromagnetic and charge disproportionation is suppressed [19].

Furthermore, the electronic conduction can be n-type or p-type, depending on the material properties and ambient oxygen partial pressure. The energy level shifts from the center of the energy gap toward the empty zone for an n-type semiconductor or the filled band for a p-type semiconductor. An n-type conductor is an electron conductor while a p-type conductor is an electron hole conductor [20].

Mixed ionic-electronic conductors exhibit both ionic and electronic conductivity. These material oxides may show both high oxygen ion conductivity due to the high oxygen vacancy concentration in the structure, and a high electronic conductivity due to the mixed-valence state. For example $La_{1-x}Sr_xBO_{3-\delta}$ in this case [21], when the B ions can take a mixed-valence state, charge neutrality is maintained by both the formations of oxygen vacancies and a change in the valence state of the B ions. The concentration of oxygen vacancies can also be increased by mild B-site ion substitution, such as [22] Cu and Ni ions which naturally take the divalent oxidation state. If the valence state of the B ions is fixed, neutrality is maintained only by the formation of oxygen vacancies. The oxides may be predominantly ionic conductors.

2.3 Perovskite synthesis

2.3.1 Solution reaction

Solution preparation of perovskite materials generally involves the use of metalloorganic compounds that are dissolved in a common solvent. General ways of making perovskite materials usually adopt mixing the constituent oxides, hydroxides and carbonates. These materials generally have a large particle size. The selection strategy of this approach frequently requires repeated mixing and extended heating at high temperature to generate a homogeneous and single-phase material.

The type of solution precursors generated by sol-gel preparations or coprecipitation of metal ions by precipitating agents such as hydroxide, cyanide, oxalate, carbonate, citrate ions etc., have been used. These gel or coprecipitated precursors can offer molecular or near molecular mixing and provide a reactive

environment during the course of subsequent heating and decomposition. Because of the improved solid-state diffusion resulting from the improved solution mixing, they need a relatively lower temperature to produce similar materials compared to the traditional methods. The solution route used will also determine the extent of intermixing of the metal species, whether formation of a network versus formation of individual inorganic phases occurs, the temperature of pyrolysis of organic species occurs, the weight loss associated with oxide formation, the densification and crystallization behavior of obtained metal oxide.

The advantages of the solution reaction methods, such as better control the stoichiometry and purity, greater flexibility in from thin films and new compositions, an easily generated porous, and an enhanced ability to control particle size.

2.3.2 Solid-state reaction

The necessary solid-state reactions proceed more rapidly and at lower temperatures. As a consequence, the desired product can be obtained with a smaller particle size and greater reactivity. Conventional processing of the perovskite-related materials uses solid-state reactions between metal-carbonates, hydroxides, and oxides. This is also known as ball milling and calcinations method. LSCF represents a typical case. Raw materials La_2O_3, $SrCO_3$, CoO_3, and Fe_2O_3 were mixed and ball-milled. After drying, then the mixed powders were calcined at 1,000 ^{o}C to remove impurities and to achieve single-phase perovskite powder. The high temperature was required to complete reaction.

2.3.3 Gas phase reaction

The deposition of perovskite films with a specific thickness and composition generally requires gas phase reaction or transport. Many physical techniques have been developed for gas phase deposition such laser ablation, dc sputtering, magnetron sputtering, electron beam evaporation, thermal evaporation and spray-pyrolysis. For example LSCF prepared form spray-pyrolysis method. Aqueous solutions of La, Sr, Co and Fe nitrates in stoichiometric amounts were spray-pyrolyzed in a heated chamber at 800 ^{o}C. The resulting fine oxide powders were collected and calcined.

2.4 Perovskite membrane preparation

Other approaches that have also been used, but less extensively, include the nitrate method, the citrate route, and the Pechini process. Those are wet chemical synthesis.

2.4.1 Wet chemical synthesis of perovskite

The most widely studied synthesis have been the chemical processing methods, which make up several procedures already applied in the synthesis of other high technology ceramics. Furthermore, a series of chemical methods, especially solution reaction or wet chemical synthesis or liquid phase synthesis, have been developed from solid-state synthesis.

In the Pechini process, a liquid mixing technique, metal nitrates are first dissolved in water. Then citric acid [an α-hydroxycarboxylic acid, $HOC(COOH)(CH_2COOH)_2$] is typically added to chelate the metal cations by forming a polybasic acid. When a polyhydroxyalcohol, most often ethylene glycol, $HOCH_2CH_2OH$, is then added, the citric acid-metal chelates will react with the ethylene glycol to form organic ester compounds. Heating of the mixture results in polyesterification and the formation of large metal/organic polymers. The process chemistry can be controlled so that a uniform solution, suitable for the deposition of homogeneous thin films, can be produced. An advantage of the Pechini method is that the viscosity and polymer molecular weight of the solution can be tailored by varying the citric acid/ethylene glycol ratio and the solution synthesis temperature. This allows for control of the thickness of the deposited films, and in the processing of perovskite gas separation membranes on porouse supports, minimization of interpenetration of the coating solution into the support. Furthermore, although the Pechini method could, in theory, be adapted to the synthesis of sulfides, carbides, or nitrides. The primary disadvantage of the Pechini method lies in the lack of control over particle size, shape, and morpgology.

The citric process has been used to fabricate a variety of multicomponent electronic ceramic materials. The citrate solution synthesis process is similar to the Pechini process, except that ethylene glycol or other polyhydroxy alcohols are not utilized. To produce citrate precursor solutions, stoichiometric amounts of the desired

metal nitrates are dissolved in water and citric acid is then added to form citrate species. This process results in solution species that have a lower organic content than in the Pechini process, and consequently, films that display less weight loss during conversion to the ceramic phase. The nitrate method simply involves the dissolution of the desired nitrates in deionized water or alcohol. The approach is thus more straightforward than the Pechini and citrate routes, but dewetting of the substrate may present a problem.

In addition, the modified citrate method was synthesized by stoichiometric nitrates dissolved into HNO_3 and citric acid was added at a ratio of, citric acid to metal ions, 2:1. The pH value of the solution was adjusted to 9 by adding $NH_3.H_2O$ and the final solution was stirred for 24 hours. Spontaneous combustion occurred when the solution was dried at 473 K.

The modifications of Pichini process have been developed (was called citate method) that involved the use from citric acid and metal nitrate before thermal decomposition. For example, the production of Sr-substituted $LaMnO_3$ perovskite powder by the amorphous citrate process, obtained the manganese citrate-nitrate precursor as shown in Equation 2.2 [23]:

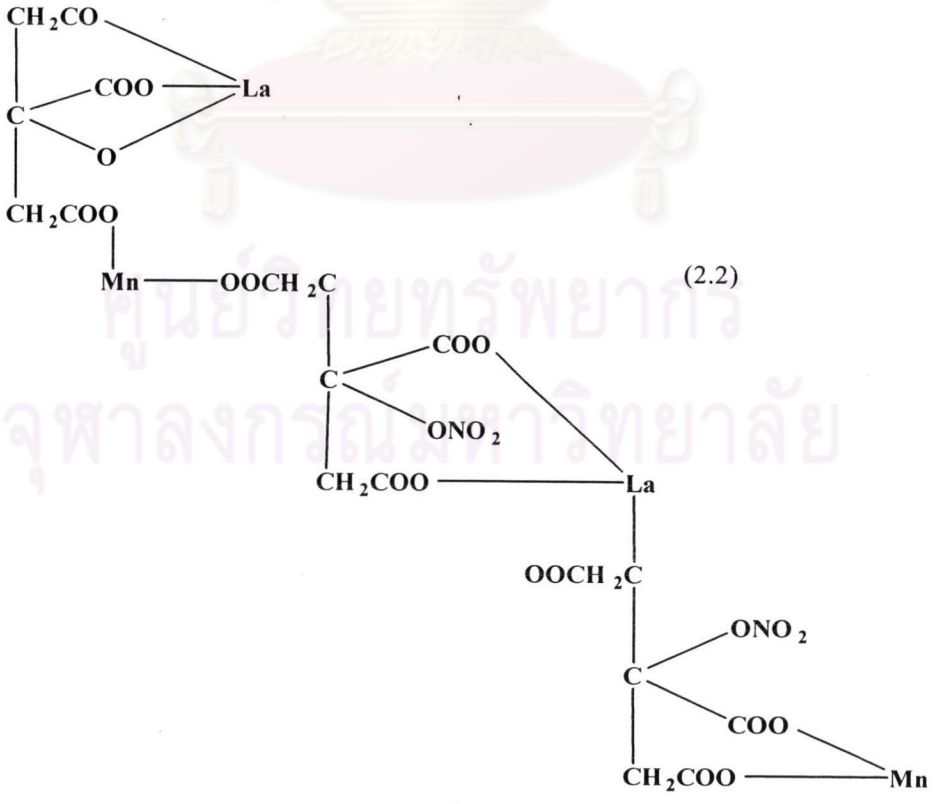

(2.2)

In the complex, the lanthanum is triply charged and replaces in normal citrate formation in the hydrogen of three –COOH groups and it replaces in the hydrogen of one –OH group and two –COOH groups. As manganese is divalent state replaces in the hydrogen of two –COOH groups while NO_2 replaces the hydrogen of one –OH group, respectively.

General, the amount of metal and citric acid should not less than equimolar. In all cases, the minimum amount of citric acid used was that necessary to bond the metals if all the NO_3^- ions were replaced. If one case, the high amount citric acid was used, Mn_2O_3 was presented from the complex; it was shown in Equation 2.3:

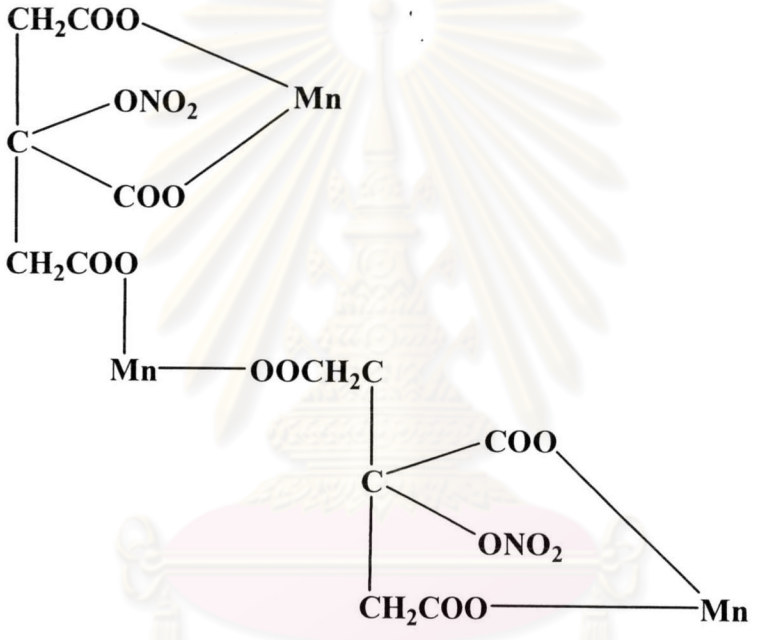

(2.3)

Another modification of the Pechini process was called the citric acid pyrolysis method [24]. The citrate process is a synthesis route which can lead to the $YBa_2Cu_3O_{7-\delta}$, the mixed metal oxides were dissolved by nitric acid. Then pH value of the dissolved nitrate solution was adjusted by $NH_3.H_2O$ and then NH_4NO_3 served as fuel. It is a particular type of sol-gel method, and offers the advantage of relative simplicity and the feasibility of the chemical compounds used in the development of the process. The method assures a great local and overall stoichiometry.

The perovskite powders made by wet chemical methods are very fine, and can be not agglomerate, which facilitates the densification process. The powders made from wet chemical methods using sintering temperature which can be lower than those made from conventional solid-state synthesis methods. By means of these

wet chemical methods, it is possible to obtain monophasic, pure, fully reacted powders with submicronic and even nanometric sizes, homogeneous and narrow size distribution, and very reactive characteristic. When comparing several techniques in wet chemical methods, liquid mix process is distinguished in the case of less energy consumption, simplest technology, and potential to get fine particles and a single-phase powder. Both adding several acids such as citric, malic acid, or etc. and adjusting the pH of aqueous solution are used to provide the fine homogeneous perovskite with the high surface area.

2.4.2 Powder sizing

Hard agglomerate in ceramic powders usually results in large interagglomerate pores after sintering. The good sinterability may be achieved when nonagglomerated powders are employed. Therefore the properties of the raw material powder are determined largely, controlled particle shape, and uniformity in chemical by the properties of the raw material powders. The particle requirements are imposed, fine particles ≤ 1 μm to compacted into porous shape and sintered at a high temperature to near theoretical density. The objective in most cases of the pressing step is to obtain high density of particle packing. Typically, the finer the powder, the greater its surface area, and the lower the temperature and shorter time for densification. Long times at sintering temperature result in increased grain growth which causes lower strength.

2.4.3 Powder compacting by uniaxial pressing

Uniaxial pressing is a single axial direction accomplished by placing the powder in to a rigid die and applying pressure along through a rigid plunger, or piston to achieve compacting. From the direct compressing into particle was results as reduces the average distance between particles and changes the shape of particles. The apparent density of a compact was controlled by particles size fractions in the various mixing materials.

To enhance the compacting, before pressing, the powder should be disaggregated by mixing the common powder with binder such as polyvinyl alcohol (PVA) to reduce the surface tension.

2.4.4 Sintering

Definitions of the sintering process can be described in term of the permanent chemical and physical change accompanied by the reduced porosity, the mechanism of grain growth, and grain bonding. This process can be accomplished by solid-state reaction or alternatively in the presence of a liquid phase. When a powdered aggregate is sintered, appeared necks form between the particles, and the aggregate may increase in density. The grain growth to the neck form is due to the transport of matter or of the counter-flow of vacancies between the particles and the pores. In crystalline powder, its transport occur by diffusion (bulk diffusion, surface diffusion, or grain boundary diffusion), whereas in amorphous materials, it occurs by viscous flow. It is shown in Figure 2.2. Therefore, the growth of grains hinders the attainment of theoretical density, and the pore's growth is also enhanced. It is essential, to retard grain growth so that densification of the compact can continue to the theoretical limit.

The sintering process can be defined by three stages to happen. The initial stages during which the necks form at points of particle contact and the particles usually center approach each other. At this stage the individual particles are still distinguishable. The intermediate stage during that the necks become large, resulting in the formation of an interconnected pore structure. The final stage during, the pores become isolated. Elimination of the interconnectivity of pores eliminates surface and vapor transport.

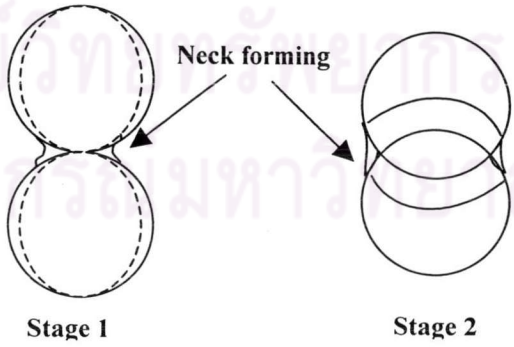

Scheme 2.1 Mechanism of sintering.

The effect of the sintering rate to the crystallization and growth processes, which occurred concurrently. The sintering rate is reduced when there is intensive

grain growth because the fine particle diffusion which forms the pores occurs toward the boundaries of individual grains. The distance which diffusion occurs with a reduction in pores is determined by the size of the crystals and d-spacing data from XRD.

2.5 Perovskite membrane concepts

2.5.1 Dense perovskite membranes for oxygen separation

Besides oxygen production, dense membranes may be applied in membrane reactors for the supply of oxygen in oxidation process. The major advantage of membrane reactors over conventional reactors are their ability to perform reaction and separation in a single step and supply in a controlled manner, for instance, the direct partial oxidation of methane to syngas, $CH_4 + 1/2O_2 \rightarrow CO + 2H_2$. It is necessary that pure oxygen is used as the oxidant. The most capital intensive part of a process unit for syngas production is the oxygen plant, so the use of mixed conducting membrane reactors, (Figure 2.3). An additional advantage of the membrane reactor approach appears to be that lattice oxygen may be a more selective form of oxygen in several partial oxidation reactions. It has been demonstrated for several reactions that electrochemically supplied O^{2-} showed better performance in terms of selectivities or conversions than molecular O_2 [25]. However, these processes required the sufficiently high temperatures, typically above about 700 ^{0}C.

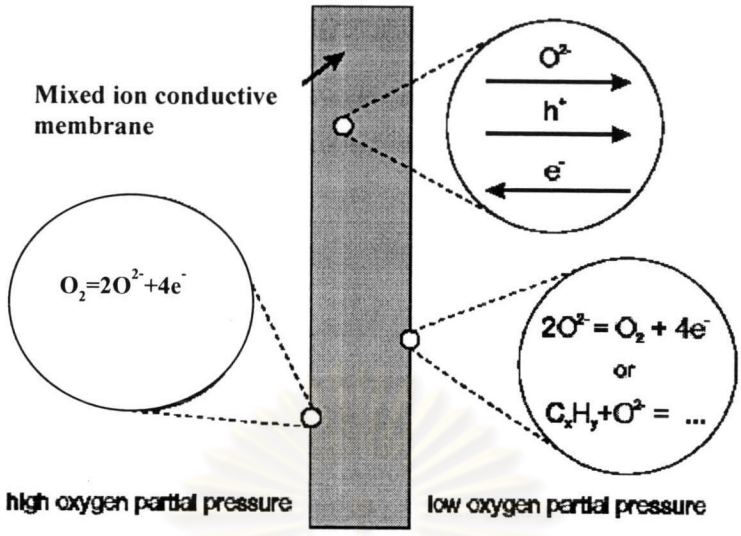

Figure 2.2 Surveys of oxygen flux and reactions in mixed-conducting membrane reactors.

2.5.2 Oxygen permeation through a mixed ionic-electronic conducting membranes

A mixed conducting membrane was placed in an oxygen partial pressure gradient, oxygen anions permeate from the high to the low partial pressure side, while overall charge neutrality was maintained by a counterbalancing flux of electrons (and/or electron holes), as depicted schematically in Figure 2.4.

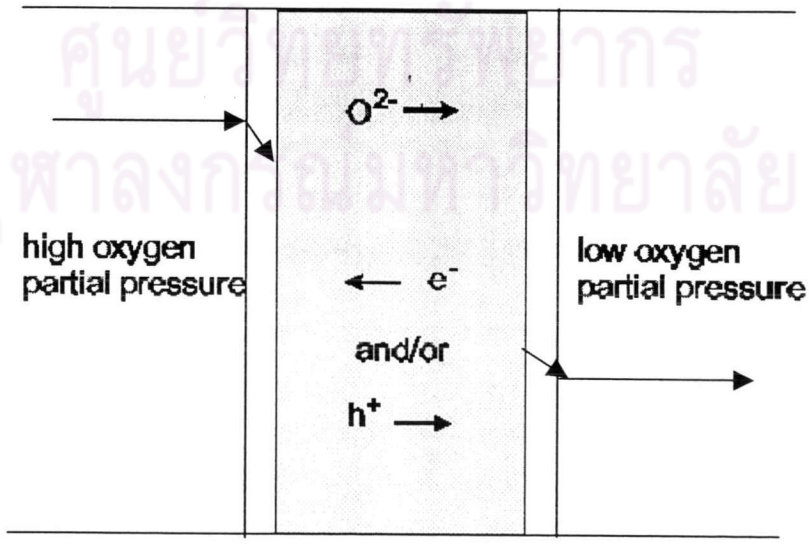

Scheme 2.2 Mechanism of the mixed ion-electron conducting membranes.

Mechanism for oxygen permeation through a mixed-conducting membrane can be described as follows [26-27]:

1. Mass transfer of gaseous oxygen from the gas phase with high oxygen partial pressure to the membrane surface.
2. Reaction between the molecular oxygen and oxygen vacancies at the membrane surface.
3. Dissociation and electron transfer, giving chemisorbed oxygen species.
4. Incorporation in membrane surface layer.
5. Diffusion of lattice defects to interior.
6. Oxygen vacancy bulk diffusion across the membrane.
7. Association and electron transfer, forming chemisorbed oxygen species.
8. Desorption from the surface.
9. Mass transfer of oxygen from the membrane surface to the gas phase with low oxygen partial pressure.

Oxygen activity drops generally occur in both interface regions and the bulk of the material. As shown in Figure 2.5, it was therefore of particular interest for practical applications to know whether the oxygen flux was limited by bulk diffusion or a surface exchange process for a certain compound. In the former case, the oxygen flux was inversely proportional to the membrane thickness. Higher permeation rates can then be achieved by reducing the thickness. In the latter case beneficial effects can only be expected from surface enlargement and modification with suitable catalytic materials on surface. A thickness L_c indicating the membrane thickness at which the oxygen flux was equally limited by bulk diffusion and surface exchange kinetics has been derived on theoretical grounds [28].

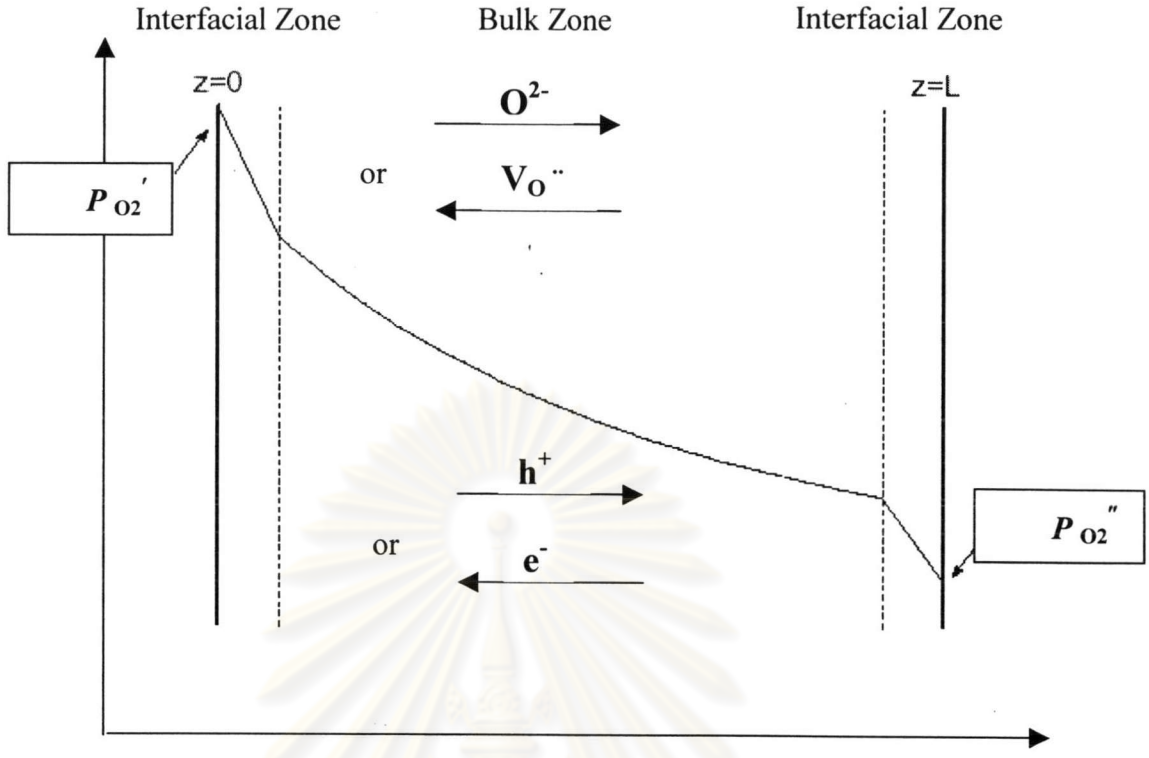

Figure 2.3 Illustration of the principle in a MIEC membrane at various zones during steady state oxygen permeation. The curve shows a possible P_{O2} Profile over the membrane. A single prime indicates air side, double prime indicates permeate side.

When the oxygen transport in a membrane is at steady state, can be calculated using the Wagner equation [29]. The thickness of the membrane is L and it was assumed for the oxygen bulk diffusion along the membrane thickness to be the rate-limiting step.

$$J_{O2} = \frac{RT}{16 F^2 L} \int_{\ln P''_{O2}}^{\ln P'_{O2}} \frac{\sigma_e \sigma_i}{\sigma_e + \sigma_i} \, d \ln P_{O2} \qquad (2.4)$$

Where σ_e and σ_i are the electronic and ionic conductivity, respectively, F the Faraday constant, R the gas constant, T the temperature, and the membrane interfaces are exposed at the higher and lower oxygen partial pressure side to atmospheres with partial pressures P'_{O2} and P''_{O2}, respectively.

The equation (2.4) can be integrates in the simplest way upon the concept those oxygen ions and electrons diffuse in a way shown in Figure 2.4. The total current density, j_{tot} (= j_e + j_{O2-}), which is the sum of the electronic and ionic partial current, can be regarded to be zero under steady state. Therefore, the actual oxygen flux expressed in terms of volume unit, J_{O2} [cm^3 (STP)/cm^2 min], can be given as follow,

$$J_{O2} = j_{O2-} / 4F$$

$$J_{O2} = \frac{RT \ (\sigma_e \sigma_i)}{16 F^2 (\sigma_e) + (\sigma_i) L} \left[\frac{\ln P'_{O2}}{P''_{O2}} \right] \qquad (2.5)$$

The first work on oxygen semi-permeable dense membranes with high ionic and electronic conductivities was reported by Teraoka et. al. [30]. A perovskite-type oxide $LaMO_3$, with Co and/or Fe on the M-site, was doped partially with Sr^{2+} on the La^{3+}-site, yielding a solid oxide solution with the general formula $La_{1-x}Sr_xCo_{1-y}Fe_yO_{3-\delta}$ (x = 0-1, y = 0-1), where δ denotes the average number of vacant oxygen sites per unit cell. δ is called the level of non-stoichimetry. In this class of materials the mechanism of charge compensation for the introduced aliovalent Sr-cations involves not only the creation of oxygen vacancies, but also the oxidation of a fraction of M^{3+} to M^{4+}, which leads to high concentrations of mobile ionic and electronic charge carriers at elevated temperatures (> 700 °C) [31]. It was shown that the oxygen permeability increased with increasing strontium content. In the later studies the influence of cation substitution in compounds $La_{0.6}A_{0.4}Co_{0.8}Fe_{0.2}O_{3-\delta}$ (A = La, Na, Ca, Ba, Sr) and $La_{0.6}Sr_{0.4}Co_{0.8}M_{0.2}O_{3-\delta}$ (M = Fe, Co, Ni, Cu) was reported [32]. Apart from fast oxygen diffusion in the bulk of the material, mixed-conducting perovskite–type oxides also exhibit a significant rate of oxygen exchange with the surrounding atmosphere [33-34], which contributes further to the high oxygen fluxes through these materials.

2.5.3 Coated disc membrane reactor

The surface morphologies of the membrane can affect the oxygen permeation flux if the permeation process is limited by the surface-exchange kinetics.

In 2002, Ishihara, *et. al.* [35] investigated the efficiency of Fe dopant for $LaGaO_3$ based on perovskite oxide as an oxygen permeating membrane for CH_4 partail oxidation. The $La_{0.7}Sr_{0.3}Ga_{0.6}Fe_{0.4}O_{3-\delta}$ powder was pressed into disk after calcinations. The obtained disk was painted on both surfaces with $La_{0.6}Sr_{0.4}CoO_3$ (LSC) slurry with the screen-printing method in order to improve the surface activity for oxygen dissociation. In order to achieving the LSGF membrane, a high oxygen permeation rate and high surface catalyst were required. High oxygen permeating rate from air to He as high as 102 μmol/min. cm^2 (2.5 cm^3 std/min.cm^2) was achieved on LSGF membrane with 0.3 mm thickness at 1000 °C.

In 2003, Lee *et al.* [36] studied the effect of surface modification by coating $La_{0.6}Sr_{0.4}CoO_{3-\delta}$ (LSC) onto $La_{0.7}Sr_{0.3}Ga_{0.6}Fe_{0.4}O_{3-\delta}$ (LSGF) and $La_{0.6}Sr_{0.4}Co_{0.2}Fe_{0.8}O_{3-\delta}$ (LSCF) membranes for oxygen permeation fluxes. It was found that the modification of both surfaces with catalytically surface-reactive LSC made an excellent oxygen-permeable Ga-doped perovskite membrane. By introducing a highly surface exchange-reactive LSC coating on the LSGF membrane, significant promotion in the oxygen fluxes could be obtained. This promotion was conspicuous if the coating layer was porous, or had larger surface area. On the contrary, the oxygen permeation flux of LSCF was not affected by surface modification.

In 2005, Kim, et. al. [37] studied the oxygen permeation of $La_{0.7}Sr_{0.3}Ga_{0.6}Fe_{0.4}O_{3-\delta}$ (LSGF) membrane coated with $La_{0.6}Sr_{0.4}CoO_{3-\delta}$ (LSC) (M1) on one side, and another side of LSGF membrane coated with NiO (M2) for the partial oxidation of methane (POM) process to syngas. From the above results, it can be concluded that LSC-LSGF membrane and NiO catalyst is very useful in the partial oxidation of methane to syngas. The oxygen permeation flux of M1 membrane (LSC coated on LSGF) at 750 and 850 °C was 0.06 and 0.13 ml/cm^2 min, respectively, and that of M2 membrane (NiO catalyst coated on the M1 membrane) at 750 and 850 °C was 0.06 and 0.11 ml/cm^2 min, respectively. From the POM experiment of the both sides, M1 and M2 coated on LSGF membrane, was carried out at 850 °C. The CH_4 conversion and CO selectivity used M1 membrane was low value of below 10 and

54 %, respectively. The CH_4 conversion and CO selectivity using M2 membrane were 15 % and 76 %, respectively. Figure 2.6 shows the experimental apparatus of partial oxidation of methane using coated membrane and gas-flow arrangement on oxygen permeation flux measuring system.

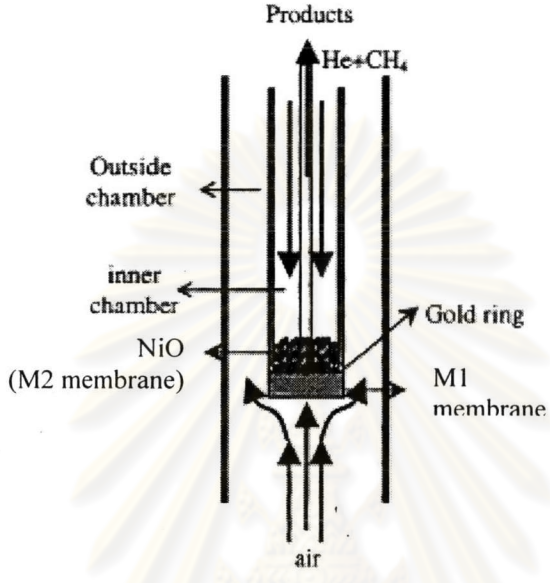

Figure 2.4 Experimental apparatus for gas-flow arrangement in oxygen permeation flux measuring system.

Several chemical and physical methods exist for depositing thin membrane top layers onto a support. Examples are sol-gel coating, sputtering and pulsed laser deposition. Van Der Haar et. al. [38] prepared the porous $La_{1-x}Sr_xCoO_{3-\delta}$ substrates (x = 0.7. 0.5 and 0.2) that were suitable for application as porous supports for thin dense mixed ionic-electronic conducting perovskite membranes. The required perovskite powders were prepared by the EDTA complexation method, followed by high temperature calcinations of the pyrolysation powder. Subsequently, the powder was homogenized by sieve. After isostatic pressing followed by sintering, the supports were 30 % porous with a mean pore diameter of around 1 μm for the composition with x = 0.7 and 0.5. As shown in Figure 2.7; the porous structure is stable at 1,100 ^{o}C. A coating of the same compositions as the support was applied to improve the surface morphology. At room temperature, the oxygen flux through the supports was 1.4 x 10^{-4} and 2.0 x 10^{-4} mole cm^{-2} s^{-1} for x = 0.7 and 0.5 respectively, at

an absolute pressure difference of 1 bar. For the composition with x = 0.2, the values of the pore diameter and oxygen flux were somewhat lower (0.8 mole cm^{-2} s^{-1}).

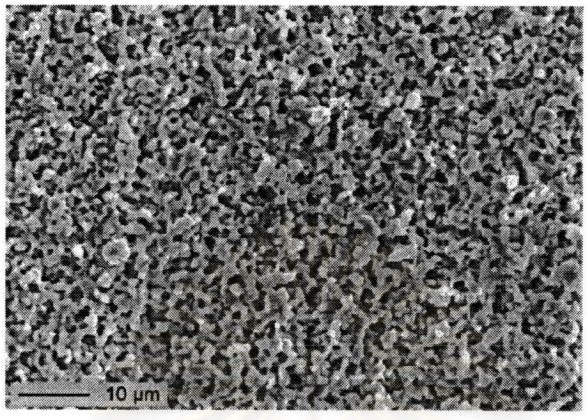

Figure 2.5 SEM picture of a coated 30%LSC support;
the coating was sintered at 1100 °C.

2.6 Oxygen permeation study and property of dense perovskite membrane

The overall rate of oxygen permeation though a dense MIEC membrane is controlled by the rate of oxygen diffusion in the membrane and the surface oxygen exchange kinetics on either side of the membrane.

In 1999, Lane, *et. al.* [39] investigated electrical, electrocatalytic and catalytic properties of $LaCoO_3$-based materials due to their high electronic and ionic conductivity values. For example, $La_{0.6}Sr_{0.4}Co_{0.2}Fe_{0.8}O_{3-\delta}$ (LSCF6428) is a mixed ionic-electronic conductor (MIEC) which displays significant and technologically useful levels of both oxygen ion and electronic conductivity. It also has the advantage of exhibiting a greater degree of stability, both mechanical and chemical, than some other mixed conducting oxides. From these reasons, the material has attracted interest for using in a wide range of application.

In 2000, Ishihara, *et. al.* [40] compared the conventional mixed electronic-oxide ionic conductor of $LaCoO_3$ and $LaGaO_3$, these $LaGaO_3$-based perovskite oxides exhibited notably high oxide ion conductivity but low electronic conductivity. Recently, the mixed electronic-oxide ionic conductors, based on $LaGaO_3$ and doped with a transition metal are used for separating air. It became evident that the electrical

conductivity was greatly improved by doping Fe, Co or Ni for the Ga site of $LaGaO_3$. In particular, Fe-doped $LaGaO_3$ exhibited a high oxygen permeation rate and stability against reduction.

In 2002, Ishihara, *et. al.* [41] studied the maximum solid solution of gallium in the perovskite-type $La_{1-x}Sr_xFe_{1-y}Ga_yO_{3-\delta}$ (x = 0.4 - 0.8; y = 0 - 0.6). It was found that the suitability of gallium in the approximate range y = 0.25 - 0.45, and y decreasing when x increases. Crystal lattice of the perovskite phases was identified as cubic. Doping with Ga resulted in increasing unit cell volume, while the thermal expansion and total conductivity of LSGF in air decrease with Ga additions. All theoretical density of LSGF ratio was higher than 91 %.

In 2000, Shao, *et. Al* [42] reported the oxygen permeation and stability of $SrCo_{0.8}Fe_{0.2}O_{3-\delta}$ (SCF), $Ba_{0.5}Sr_{0.5}Co_{0.8}Fe_{0.2}O_{3-\delta}$ (BSCF) oxide, using a combined citrate-EDTA complexing method. The O_2-TPD and XRD results showed that the introduction of barium into SCF could effectively suppress the oxidation of Co^{+3} and Fe^{+3} to higher valence states of Co^{+4} and Fe^{+4} in the lattice, and could stabilize the perovskite structure under lower oxygen partial pressures. Oxygen permeation experiment indicated that BSCF membrane has also higher oxygen permeation flux than that SCF under air/He oxygen partial gradient. At 950 °C, the permeation flux reached about 1.4 ml/cm^2 min through 1.80 mm thickness BSCF membrane. The permeation flux and phase structure of BSCF membrane were very stable at higher than 850 °C. The phase transition was found to be reversible at high temperatures. BSCF is a promising material for using in oxidation membrane reactors at operation temperatures higher than 850 °C. Substitution of proper amount of Sr^+ in the A-site of SCF by larger metal ion Ba^{2+} led to obvious improvement in the phase stability of this material at high temperature.

2.7 Effect of A-site or B-site substituted on the ABO_3 perovskite structure

In 1994, Ishihara, *et. al.* [43] reported that the Sr substitution could increase the electrical and ionic conductivity of $LaGaO_3$ based perovskites and the ionic conductivity, σ_i, by increasing amount of Sr additives. The attained maximum limit of the solid solution is x = 0.1 in $La_{1-x}Sr_xGaO_3$. Since the number of oxide vacancies increased with increasing amount of Sr dopant. Larger numbers of oxide vacancies

were theoretically obtained and, as a result of, higher oxide ion conductivity was enhanced when amount of Sr dopant increased. However, impure crystal phases such as $SrGaO_3$ and La_4SrO_7 were detected above x = 0.1 in $La_{1-x}Sr_xGaO_3$ by XRD analysis.

In 2004, Yeyongchaiwat, *et. al.* [44] studied the influence of amount of Ga doped for obtaining the single phase, where study on two series of oxide, with the fixed components, $La_{0.4}Sr_{0.6}Ga_{1-y}Fe_yO_{3-\delta}$ and $La_{0.6}Sr_{0.4}Ga_{1-y}Fe_yO_{3-\delta}$ (y = 0.4, 0.6, 0.8) used the modified citrate method. By increasing the amount of Fe from 60 % to 80 % in $La_{0.4}Sr_{0.6}Ga_{1-y}Fe_yO_{3-\delta}$ and $La_{0.6}Sr_{0.4}Ga_{1-y}Fe_yO_{3-\delta}$, single phase was obtained and theoretical density was higher than 90 %.

In 2004, Wang, *et. al.* [45] prepared $La_{1-x}Sr_xFeO_3$ (x = 0.0 - 1.0) by sol-gel method. The XRD patterns revealed the presence of a single perovskite structure for substitutions $0 \leq x \leq 0.3$, and Fe_2O_3, $SrCO_3$, $SeFeO_3$ phases were observed for substitutions $x > 0.3$. The results of activity test indicated that the combustion of methane could take place at low temperature around 400 °C when $La_{1-x}Sr_xFeO_3$ was used as the catalyst. Partial substitution of La with Sr increased the activity. It was found that the catalytic activity could be well correlated with the product of the specific surface area and the atomic ratio of Fe to $LaSrO_3$ on the catalyst surface. An optimal substitution fraction (x = 0.5) exists in the $La_{1-x}Sr_xFeO_3$ catalysts.

In 2005, Augustin, *et. al.* [46] studied the effect of La^{3+} substituted nanocrystalline $La_xSr_{1-x}FeO_3$ (x = 0.0, 0.2, 0.4, 0.6, 0.8) which has been prepared by citrate combustion method. The XRD patterns showed the high crystalline nature of the synthesized compounds without any impure phase. The lattice constant and cell volume were increased with increasing the molar substitution of La^{3+} on Sr^{2+} due to the difference in ionic radii (La^{3+} = 1.36 A°, Sr^{2+} = 1.25 A°). A phase transition from cubic to orthorhombic had been observed with increasing La^{3+} substitution. The compounds $La_{0.4}Sr_{0.6}FeO_3$ gave the maximum electrical conductivity.

2.8 Effect of temperature on crystal structure development

In 1998, Zhang, et. al. [47] reported the effects of microstructure on the oxygen permeation in $SrCo_{0.8}Fe_{0.2}O_{3-\delta}$ (SCF) and $La_{0.2}Sr_{0.8}Fe_{0.8}Cr_{0.2}O_{3-\delta}$ (LSFC) by using disk samples fabricated under different processing conditions. The

microstructure of LSFC2882 remained unchanged when the sintering temperature was increased from 1,300 to 1,450 °C, but the average grain size of SCF increased considerably when the sintering temperature was increased from 930 °C to 1,200 °C. The change in grain size was found to have a strong effect on the oxygen permeation flux in SCF. The oxygen permeation flux of SCF was decreased, which increased considerably as the grain size. This indicates that the contribution of the grain boundary diffusion to the steady state oxygen flux in SCF is substantial and grain boundaries provide faster diffusion paths in oxygen permeation though the sample.

In 2003, Tan, et. al. [48] examined microstructure and oxygen permeation performance of $Ba_{0.5}Sr_{0.5}Co_{0.8}Fe_{0.2}O_{3-\delta}$ (BSCF oxides) oxides using different preparation methods. The oxide powders were synthesized by solid state reaction, modified citrate and citrate-EDTA complexing method. Powder synthesized by different methods can produce different grain morphologies although the particle size distributions are nearly the same. The membrane preparations by using powders prepared from different method have different microstructures, which influence their oxygen permeation performance.

In 2004, Xu, *et. al.* [49] investigated the influence of sintering temperature on microstructure and mixed electronic-ionic conduction properties of $La_{0.6}Sr_{0.4}Co_{0.8}Fe_{0.2}O_3$ ceramics in the range 1,100-1,250 °C. The results confirm the crucial role of sintering temperature on microstructure and mixed conduction properties. As a result, the development of densification at 1,100 - 1,200 °C is responsible for the improvement of the mixed conduction properties. Raising the sintering temperature further above 1,200 °C resulted in degradation of the mixed conduction properties due to the generation of excessive liquid. The results demonstrate that it is crucial to adequately control sintering temperature to yield desired microstructure and mixed conduction properties. The preferred sintering temperature was ascertained to be 1200 °C for $La_{0.6}Sr_{0.4}Co_{0.8}Fe_{0.2}O_3$ ceramics in terms of mixed conduction properties. The specimen sintered at 1,200 °C exhibited an electrical conductivity of 1.26 x 10^3 Ω^{-1} cm^{-1} and an oxygen ionic conductivity of 3.73 x 10^3 Ω^{-1} cm^{-1} at 800 °C.

In 2005, Petitjean, *et. al.* [50] studied the crystallographic changes between room temperature (RT) and 700 °C of $(La_{0.8}Sr_{0.2})(Mn_{1-y}Fe_y)O_{3-\delta}$ perovskites with y = 0.2, 0.5,0.8, and 1.0 from XRD. For y = 0.2, it was found that the rhombohedral

symmetry was preserved in the whole temperature range. For y = 1.0, a transition of orthorhombic symmetry was occurred at 290 °C. The compounds with y = 0.5 and 0.8 were found to be diphasic at RT by combination of both rhombohedral and orthorhombic symmetries. They became only rhombohedral at 80 and 160 °C, respectively. This reversible transition is discussed in terms of iron concentration, vacancy diffusion and oxidation state.

2.9 Oxygen content determination in perovskite by using thermogravimetric analysis

Various methods have been used to investigate the oxygen exchange kinetics. Among these methods, using the commercial thermogravimetric instrument to study the oxygen kinetics seems to be one most conventional method. Kishio et. al. [51] studied the chemical diffusion of oxygen in $YBa_2Cu_3O_{7-\delta}$ (YBC) and Zhu et. al. [52] studied the oxygen desorption activation energy of YBC by the thermogravimetry. Hu et. al. [53] measured the weight difference in oxygen and nitrogen of YBC. Figure 2.8 shows for the change of δ with temperature in oxygen and nitrogen, respectively. It was found that, the distance between two temperature steps 50 °C and the temperature step start at 400 °C. At every temperature step, 30 minutes was maintained to ensure δ reaches its equilibrium with temperature. When the sample was in oxygen at 400 °C, its weight has a little increase, indicating that the sample originally has a little oxygen vacancy; therefore, scale of the oxygen content at 400 °C corresponds to $\delta = 0$. In this study, permeation properties and surface reaction rate constant of YBC following the method of Zeng and Lin [54] used a transient thermogravimetric method to study the oxygen permeation properties of $La_{0.2}Sr_{0.8}CoO_{3-\delta}$ and obtain the lumped surface reaction rate constant. This transient thermogravimetric experiment was performed on a homemade statistic adsorption instrument at temperature region 500-800 °C.

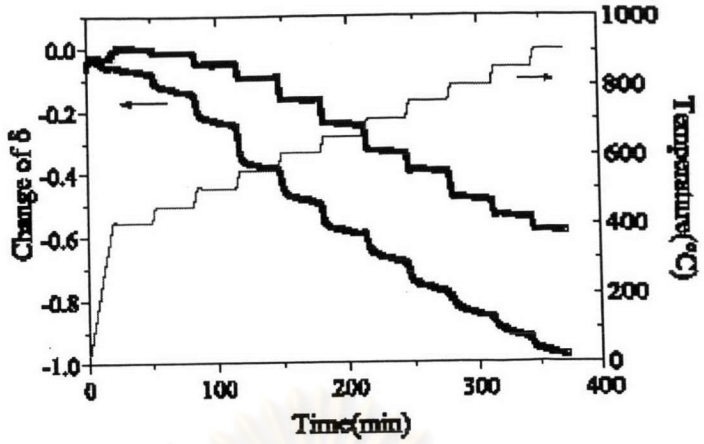

Figure 2.6 Increase of oxygen vacancy concentration (δ) with temperature increase in oxygen and nitrogen flow, respectively.

A simple correlation between the oxygen permeation flux and rate constants measured by the transient thermogravimetric analysis (TGA) method is given. The oxygen permeation fluxes calculated from data measured by present TGA method are consistent with the data measured by the permeation method. The TGA method is found particularly useful for studying the surface reaction rates of oxygen permeation through thin mixed-conducting ceramic membranes.